

Analytical Methods

Accepted Manuscript

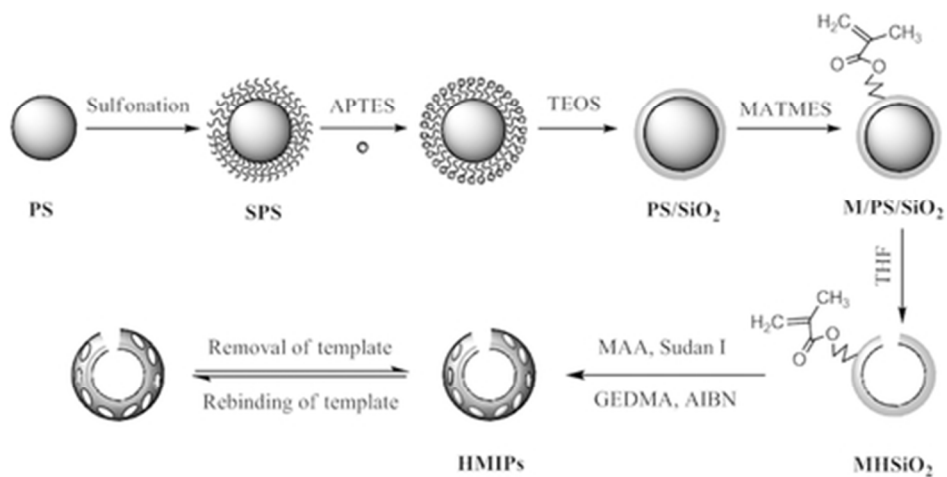


This is an *Accepted Manuscript*, which has been through the Royal Society of Chemistry peer review process and has been accepted for publication.

Accepted Manuscripts are published online shortly after acceptance, before technical editing, formatting and proof reading. Using this free service, authors can make their results available to the community, in citable form, before we publish the edited article. We will replace this *Accepted Manuscript* with the edited and formatted *Advance Article* as soon as it is available.

You can find more information about *Accepted Manuscripts* in the [Information for Authors](#).

Please note that technical editing may introduce minor changes to the text and/or graphics, which may alter content. The journal's standard [Terms & Conditions](#) and the [Ethical guidelines](#) still apply. In no event shall the Royal Society of Chemistry be held responsible for any errors or omissions in this *Accepted Manuscript* or any consequences arising from the use of any information it contains.



Graphical abstracts
39x19mm (300 x 300 DPI)

Synthesis, characterization and evaluation of hollow molecularly imprinted polymers for Sudan I

Dong Ren^a, Jiang He^{*a}, Haixia Zhang^{ab}

A novel strategy was developed to prepare hollow molecularly imprinted polymers (HMIPs) with thin and solid shell, in which introduced soft polystyrene core and hard inner shell of SiO₂, and combined surface molecular imprinting of Sudan I and in situ polymerization. The HMIPs possessed good morphological stability without deformation and broken owing to the existing of SiO₂. The thin imprinted coating (50 nm) of HMIPs ensured the faster mass transfer and the higher efficiency of active sites utilization during the adsorption. What's more, it was successfully applied as solid-phase extraction (SPE) sorbent for selective adsorption of Sudan I in chilli powder samples, and the satisfied recoveries were obtained in the range of 95-108% with the spiked samples.

1. Introduction

In recent years, molecular imprinting has been considered as a promising method for synthesizing the materials with memory of the shape and size for template molecule. The materials obtained were named as molecular imprint polymers (MIPs) [1-5]. Owing to the easy preparation, good stability and recognition properties, MIPs have been applied in many fields for the separation and enrichment of target molecules, especially acted as solid phase extraction (SPE) sorbents in sample pretreatment [6-8]. In order to meet the needs in practical applications, various synthesis strategies have been developed, including bulk polymerization, precipitation polymerization, and suspension polymerization etc. Although the MIPs prepared using the above methods exhibited good binding affinity and specificity toward target molecules, they involved in some shortcomings, such as incomplete template removal, low utilization ratio of binding sites, and slow mass transfer because of their highly cross-linked nature [9].

To overcome the above shortages mentioned, methods such as surface imprinting [10], porous imprinting [11], and hollow imprinting have been developed [12-18]. The hollow imprinting polymers (HMIPs) have aroused extensive attention especially, owing to their larger specific surface area, higher utilization ratio of binding sites, and faster mass transfer. There are two main methods for synthesis of HMIPs with sacrificing soft or hard core, respectively. For method with sacrificing soft core, divinylbenzene (DVB) [12-14] was usual as cross-linking agent and polystyrene (PS) particle as core. Because the dissolving and removal of the core was accompanied with its swelling, which led to the collapse of the polymer outside, the thicker imprinting shell had to be made. However, the thick imprinting shell led to low mass transfer and low utilization ratio of binding sites. For method with sacrificing hard core, SiO₂ or TiO₂ were usual as the core [15-18]. With this kind of method, thin imprinting shell (50-80 nm) could be obtained. But, the thin shell was fragile and easy to be broken.

Sudan dyes (Their structures are shown in Fig. S1, ESI†) are phenyl-azoic derivatives, with an orange-red appearance [19]. Due to azo dyes considered to be genotoxic carcinogen and mutation for humans, their presence are not permitted in foodstuffs for any purpose at any level [20]. Sudan I was the most common dye used illegally as additives to enhance the gaily-colored appearance of food products containing chilli, curry, curcuma, palm oil and so on [21,22]. Therefore, it is important to inspect the presence of the Sudan I in foodstuffs. A lot of analytical methods have been developed for the determination of Sudan dyes [23-26]. Owing to the complexities of sample matrixes and the low levels of Sudan I, sample pretreatment and enrichment processes have become the crucial steps in the analytical procedures [27-28].

Up to now, some MIPs for Sudan I had been prepared with different methods [28-33]. Among them, no HMIPs have been prepared. In this work, it was the first time to design a new approach to prepare a novel HMIPs with thin and solid MIPs shell. We used PS/SiO₂ particles as core and only PS part was sacrificed. It is to say, SiO₂ part was kept in the HMIPs as the support, which made it possible to get a thin but solid MIPs shell. The HMIPs prepared was not only avoided the deformation and broken, but also offered high utilization ratio of binding sites and faster mass transfer. The HMIPs were fully characterized and evaluated by scanning electron microscopy (SEM), transmission electron microscopy (TEM), thermogravimetry analysis (TG) and Fourier transform infrared spectrometer (FT-IR). Their molecular recognition capacities were also investigated in detail. The HMIPs was further used as SPE sorbents to selective adsorb and enrich Sudan I from chilli power samples and the satisfied recoveries were obtained.

2. Experimental

2.1 Reagents and chemicals

Methacrylic acid (MAA), acetonitrile (ACN), tetrahydrofuran (THF), styrene, ammonia (25-28%), toluene, and chloroform were from Tianjin Guangfu Fine Chemical Research Institute (Tianjin, China). Ethylene glycol dimethacrylate (EGDMA), tetraethoxysilane (TEOS), 3-methylacryloxypropyl trimethoxysilane (MATMS), and 3-aminopropyl triethoxysilane (APTES) were purchased from Alfa Aesar (Beijing, China). Potassium peroxydisulfate ($K_2S_2O_8$) and Azo-bis-isobutyronitrile (AIBN) were obtained from Chemistry Reagent Factory of Chinese Fuchen (Tianjin, China). Sudan I-IV were purchased from Sinopharm Chemical Reagent Co. Ltd (Shanghai, China). All the chemicals above were of analytical grade. Chilli powder samples were bought from a local market in Lanzhou, China. Ultra pure water was used throughout the whole experiments.

2.2 Instruments

The morphologies of prepared polymers were observed by a JEM-1200EX TEM (Tokyo, Japan), and an S-94 4800 SEM (Hitachi, Japan). Infrared spectra were collected on a Nicolet 20 NEXUS 670 FT-IR spectrometer (Ramsey, MA, USA). The TG analysis over 50-800 °C was obtained by a STA PT1600 Thermal Analyzer Instruments (Linseis, Germany) with the heating rate of 10 °C min⁻¹ under N₂.

The chromatographic analytical system consisted of a Model 210 HPLC pump and a UV-Vis detector (Varian Prostar, USA). All separations were carried out on a C₁₈ column (Dikma Technologies, 250×4.6 mm, 5 μm). The UV-Vis detector was operated at 478 nm for Sudan I and 520 nm for Sudan II-IV. The optimal HPLC conditions for Sudan dyes were as follows: mobile phase: ACN-water 95:5 (v/v); flow rate: 1.0 mL min⁻¹; room temperature; injection volume: 20 μL [33].

2.3 Preparation of hollow molecularly imprinted polymer for Sudan I (HMIPs)

2.3.1 Synthesis of PS/SiO₂ spheres

First, monodisperse polystyrene (PS) particles (500 nm in diameter) were synthesized by emulsifier-free emulsion polymerization method according to the previous report with some modification [9]. Styrene monomer (4.0 g) was added to 60 mL of water under stirring for 10 min at 70 °C in N₂ atmosphere. And then 4.0 mL of $K_2S_2O_8$ aqueous solution (23.0 mg mL⁻¹) was added. After the reaction was refluxed for 24 h, the monodisperse PS spheres were obtained after centrifugation (8000 rpm, 10 min) and washing with water for several times.

Then, the PS spheres were dispersed in 60 mL of concentrated sulfuric acid (H₂SO₄), the sulfonation reaction was allowed to take place at 40 °C for 4 h. The obtained Sulfonated PS (SPS) spheres were purified by repeat washing with water and ethanol until the pH reached to 6.0.

The obtained spheres were dispersed in 50 mL of water again and 0.5 mL of APTES monomer was added. The mixture was kept stirring for 12 h at 25 °C, and then centrifuged and washed with ethanol to remove the unreacted APTES. The precipitate obtained was dispersed in a solution consisted with 50 mL of ethanol, 10 mL of ammonia and 10 mL of water, followed by adding 1.5 mL of TEOS dropwise under stirring. The reaction was kept for 3 h at 50 °C. The PS/SiO₂ spheres were obtained after centrifugation and washing with ethanol [34].

2.3.2 Synthesis of MATMS functionalized hollow SiO₂ (MHSiO₂)

The surface of SP/SiO₂ spheres was modified further with MATMS by following. The SP/SiO₂ spheres were dispersed in the solution with 100 mL of ethanol, 1.0 mL of ammonia and 0.2 mL of MATMS, and then the mixture was stirred for 24 h at 25 °C. After the products were centrifuged and washed with ethanol for several times, they were dispersed in THF for 2-3 h to dissolve the PS core. The final products MHSiO₂ were dried in vacuum at 50 °C for 24 h.

2.3.3 Synthesis of HMIPs for Sudan I

Typically, Sudan I (24.8 mg, 0.1 mmol) and MAA (34.5 μL, 0.4 mmol) were added in 24 mL of toluene and stirred for 8 h in dark to finish the pre-polymerization. Then under stirring, 375 μL (2.0 mmol) of EGDMA, 20 mg of AIBN, 1 mL of chloroform and 160 mg of MHSiO₂ spheres were added in the pre-polymerization solution. After deoxygenized with N₂ for 5 min, the polymerization was undertaken at 60 °C for 12 h under N₂ protection. The products were collected and washed with ACN.

The template molecules were removed by Soxhlet extraction in methanol-acetic acid solution (90:10, v/v) until no Sudan I could be detected by HPLC from the HMIPs. The HMIPs were finally dried in vacuum for 24 h at 50 °C. The preparation route was shown in Scheme 1.

For comparison, non-imprinted hollow polymer (HNIPs) was prepared with the same procedure except for the presence of Sudan I.

(Scheme 1)

2.4 Estimation of recognition properties of HMIPs

In order to evaluate the binding capacity of the HMIPs, a static adsorption experiment was performed first by placing 20 mg of HMIPs into 2 mL of ACN containing Sudan I with various concentrations. The mixture were shaken for 24 h at room temperature, then the supernatant solution was collected, the concentrations of Sudan I

110 were detected by HPLC method. Every test was done for parallel three times and the experimental data were the
111 mean values of the results.

112 The data of the static adsorption experiment were further processed with the Langmuir isotherm models (Eq. (1))
113 and Freundlich isotherm models (Eq. (2)) to estimate the binding parameters of HMIPs prepared [35, 36]. Q ($\mu\text{mol g}^{-1}$)
114 was the amount of Sudan I bound to MIPs at equilibrium, Q_{max} ($\mu\text{mol g}^{-1}$) was the maximum binding capacity,
115 C_{free} ($\mu\text{mol mL}^{-1}$) was the equilibrium concentration of Sudan I, K_L ($\text{mL } \mu\text{mol}^{-1}$) was the Langmuir binding
116 coefficient, K_F ($(\mu\text{mol g}^{-1}) (\text{mL } \mu\text{mol}^{-1})^{1/n}$) was the Freundlich binding coefficient and n was the Freundlich binding
117 constant.

$$\frac{C_{\text{free}}}{Q} = \frac{C_{\text{free}}}{Q_{\text{max}}} + \frac{1}{K_L Q_{\text{max}}} \quad (1)$$

$$\log Q = \log K_F + \frac{1}{n} \log C_{\text{free}} \quad (2)$$

119 Then a dynamic adsorption test for Sudan I was carried out. 200 mg of HMIPs were dispersed in 20 mL of ACN
120 containing 1.20 $\mu\text{mol mL}^{-1}$ or 0.16 $\mu\text{mol mL}^{-1}$ of Sudan I, respectively. The mixtures were shaken at 25 °C in a
121 thermostat oscillator. At different time interval the concentration of Sudan I in solution was determined. The data
122 were further processed with pseudo-first-order kinetic model (Eq. (3)) and pseudo-second-order kinetic model (Eq.
123 (4)). Where Q_e ($\mu\text{mol g}^{-1}$) was the equilibrium uptake, Q_t ($\mu\text{mol g}^{-1}$) was the adsorption capacity at different time,
124 k_1 (min^{-1}) was the first-order rate constant, k_2 ($\text{g } \mu\text{mol}^{-1} \text{min}^{-1}$) was the second-order rate constant, t (min) is the
125 adsorption time, and v ($\mu\text{mol g}^{-1} \text{min}^{-1}$) was initial sorption rate ($v=k_2 Q_e^2$).
126
127

$$\log(Q_e - Q_t) = \log Q_e - \frac{k_1 t}{2.303} \quad (3)$$

$$\frac{t}{Q_t} = \frac{1}{k_2 Q_e^2} + \frac{t}{Q_e} \quad (4)$$

128
129
130 Third, the selectivity of HMIPs towards Sudan I was evaluated with a series of experiments on HMIPs and
131 HNIPs, using 0.40 $\mu\text{mol mL}^{-1}$ of Sudan I and its structural analogs (Sudan II-IV). The experiment process was
132 same as the static adsorption experiment.

133 2.5 Analysis of chilli powder samples

134 Chilli powder samples were used to demonstrate the applicability of the HMIPs to enrich Sudan I from
135 complicated matrices. Extraction of Sudan I from 2.0 g of spiked or non-spiked chilli powder was carried out by
136 adding 4 mL of *n*-hexane. The mixture was shaken for 5 min and the supernatants were collected. The residue was
137 washed with *n*-hexane for another twice. The extracts were pooled together, filtrated with 0.22 μm filter and
138 diluted to 25.0 mL.

139 An empty SPE cartridge was packed with 400 mg of the HMIPs, which was conditioned sequentially with 5 mL
140 of methanol and 10 mL of *n*-hexane at a flow rate of 1.0 mL min^{-1} , and then the cartridge was loaded with the
141 prepared samples at a flow rate of 5 mL min^{-1} . After loading, the column was washed with 4 mL of methanol at 1
142 mL min^{-1} . Finally, the elution was performed by passing 6 mL of methanol-acetic acid solution (90:10, v/v) [12].
143 The eluant was collected and evaporated under N_2 . The residue was dissolved in 200 μL of mobile phase for HPLC
144 analysis.

145 3. Result and discussion

146 3.1 Preparation of HMIPs

147 In our preparation, how to coat PS sphere with SiO_2 shell was the key step. Without the synthesis of SPS spheres,
148 it was failed to form the PS/ SiO_2 spheres. So the PS sphere was first sulfonated with H_2SO_4 to form sulfo groups
149 on its surface and then APTES monomer was introduced through the bonding between the sulfo groups and the
150 amino groups, which led further to the successful formation of SiO_2 shell.

151 The ratio of template molecules and functional monomers, the type of cross-linkers and the kind of solvents
152 were taken into consideration in the preparation of HMIPs. MAA was chosen as the functional monomer because it
153 could form hydrogen bond with Sudan I. The molar ratios of template molecule, functional monomer and
154 cross-linker were set at 1:4:20 according to the references [30, 33]. The HMIPs were prepared in toluene or
155 chloroform to investigate the influence of solvent. As can be seen from table 1, toluene was superior to chloroform
156 as the solvent for the synthesis of HMIPs for Sudan I.

1
2
3 157 (Table 1)

4 158 **3.2 Characterization of the HMIPs**

5
6 159 The SEM and TEM images of PS/SiO₂, MHSiO₂, HMIPs were shown in Fig. 1. As shown in Fig. 1A and Fig. 1a,
7 160 the PS/SiO₂ spheres with an average diameter of 550 nm were uniform and their surface was smooth. Fig. 1B and
8 161 Fig. 1b showed the images of the MHSiO₂ spheres, which were obtained by removing the PS core with THF, and
9 162 the shell thickness of the MHSiO₂ was about 15 nm. A hole was present on the SiO₂ shell. In Fig. 1C and Fig. 1c,
10 163 the MIP coating was successfully synthesized onto the MHSiO₂ surface and the thickness of the imprinted shell
11 164 was estimated about 50 nm. It could be seen the HMIPs were rigid and kept perfect spherical shape without
12 165 breakage and deformation. The hole on the SiO₂ sphere was survived, which ensured that the template molecules
13 166 could enter the imprinted cavities from both sides of the polymer spheres.

14 167 (Fig. 1)

15 168 FT-IR spectra were employed to ascertain the successful synthesis of materials (Fig. S2, ESI[†]). In the spectrum
16 169 of SPS particles (Fig. S2a), the typical PS absorption bands at 1600, 1492, 1451, 755, and 698 cm⁻¹ were clearly
17 170 seen [37]. The band at 1068 cm⁻¹ was ascribed to the -SO₃H group, confirming that the PS spheres were doped
18 171 with -SO₃H directly [34]. In the spectrum of PS/SiO₂ particles (Fig. S2b), the asymmetrical stretching vibration
19 172 peak of siloxane bond (Si-O-Si) was found at 1087 cm⁻¹; and the peaks at 960 cm⁻¹ and 3418 cm⁻¹ were from the
20 173 stretching vibration of the hydroxyl group in Si-OH, which confirmed that the SiO₂ shell was successfully
21 174 modified on the surface of PS. The peak of C=O at 1713 cm⁻¹ and the C-O asymmetric stretching vibration of
22 175 MATMS at 1192 cm⁻¹ in M/PS/SiO₂ spectrum (Fig. S2c) showed the MATMS had been grafted onto the surfaces
23 176 of the PS/SiO₂. The typical bands of PS were disappeared in the spectrum of MHSiO₂ (Fig. S2d), which indicated
24 177 that the PS core was removed by THF successfully. HMIPs and HNIPs exhibited strong absorption bands around
25 178 1728 cm⁻¹, 1253 cm⁻¹, and 1454 cm⁻¹, which were assigned to the C=O stretching vibration from MAA and
26 179 EGDMA, the C-O symmetric stretching vibration and the CH₂ stretching vibration from EGDMA, respectively
27 180 [39,40].

28 181 TG analysis results were obtained (Fig. S3, ESI[†]). PS/SiO₂ could be stable below 371 °C. When the temperature
29 182 was increased to 800 °C, the weight loss was increased to 77.6%, which was resulted from the loss of PS core. For
30 183 the HMIPs and HNIPs, the weight loss of water below 265 °C was observed. In the range of 265-465 °C, the
31 184 polymers on the surface of HMIPs and HNIPs were decomposed seriously. At 800 °C, the residue amounts (SiO₂)
32 185 were only 5.7% and 7.3% for HMIPs and HNIPs, respectively.

33 186 **3.3 Binding profiles of the HMIPs**

34 187 Fig. 2 showed the adsorption isotherm of HMIPs and HNIPs for Sudan I in ACN. It can be noted that the
35 188 adsorption capacities of HMIPs and HNIPs increased with the increased initial concentration of Sudan I from 0 to
36 189 2 μmol mL⁻¹. The imprint factors α ($Q_{\text{HMIPs}}/Q_{\text{HNIPs}}$) were near each other at the different initial concentrations,
37 190 which were in a range of 2 to 3.

38 191 (Fig. 2)

39 192 The Langmuir and Freundlich isotherm models were employed for studying the adsorption thermodynamics
40 193 data (Table 2). The linear coefficients (R^2) were close each other, which indicated that both the monolayer and
41 194 multilayer adsorption might be coexisted in the complex adsorption process. The maximum adsorption capacities
42 195 (Q_{max} , μmol g⁻¹) were calculated to be 12.5 for the HMIPs and 6.32 for HNIPs. The Freundlich binding constants (n)
43 196 of the HMIPs and HNIPs were 1.51 and 1.39, respectively. n was larger than 1, indicating the adsorption was easy
44 197 to occur. The Freundlich binding coefficient (K_F , (μmol g⁻¹) (mL μmol⁻¹)^{1/n}) of the HMIPs (10.35) was about 2
45 198 times of the HNIPs (4.05), certifying further that the HMIPs possessed higher adsorption capacity than the HNIPs
46 199 owing to the imprinting effect.

47 200 (Table 2)

48 201 Fig. 3 depicted the kinetic curve of Sudan I on the HMIPs and HNIPs. The adsorption amount of HMIPs and
49 202 HNIPs increased sharply during the first 10 min for the initial concentration of 0.16 μmol mL⁻¹ or 60 min for 1.21
50 203 μmol mL⁻¹ and then reached stable, which meant the equilibration time was depended heavily on the initial
51 204 concentration. Compared with the similar hollow MIPs materials reported in references, it was found the new
52 205 HMIPs prepared in the work had the advantage of having faster mass transfer rate compared with [12, 13] and not
53 206 crushed easily compared with [17, 18]. The detailed comparison with the references was summarized in table 3.

54 207 (Fig. 3)

55 208 (Table 3)

56 209 Pseudo-first-order kinetic model and pseudo-second-order kinetic model [41] were used to study the kinetics
57 210 procedure. For both HMIPs and HNIPs, the experimental data were well fitted to the pseudo-second-order model
58 211 with a correlation coefficient ($R^2 > 0.993$). The Q_e value (μmol g⁻¹) for the HMIPs was calculated as 11.5, which
59 212 was near 2 times higher than of the HNIPs (6.16). The ν value (μmol g⁻¹ min⁻¹) for HMIPs was 0.695, which was
60 213 higher than from the HNIPs (0.432), suggesting that the HMIPs had a higher adsorption rate.

214 The Q_e value (μmol g⁻¹) calculated from Freundlich isotherm model was 12.5 and 11.5 from

215 pseudo-second-order kinetic model, which indicated that 92% of binding sites were utilized in the adsorption
216 procedure. The very high utilization ratio of binding sites resulted to the larger adsorption capacity compared with
217 the other HMIPs with PS core [16,17].

218 3.4 Selectivity of the HMIPs

219 Solvent could affect the interaction between the template molecules and HMIPs. Pure ACN, 90% and 40% ACN
220 in water solution were chosen as the solvents to carry out the selectivity tests. H₂O could destroy the special
221 binding sites by reducing the hydrogen bond between the binding sites and the template molecules and led to the
222 decreased imprint factor α (1.5 times) for HMIPs but the increased adsorption capacity was obtained (1.6 time) for
223 both HMIPs and HNIPs owing to the decreased solubility of Sudan I in the solution.

224 Sudan dyes had the very similar structures and Fig. 4 showed the adsorption capacities of the HMIPs and HNIPs
225 to Sudan I-IV in ACN. The HMIPs showed the selectivity factors k (the ratio of $\alpha_{\text{Sudan I}}$ and $\alpha_{\text{other Sudan dyes}}$) were
226 between 1.5-2.0, which was larger than our previous report (no more than 1.5) [33]. The higher k values to the
227 substances with similar structures meant the better discernment capacity of the HMIPs, which maybe benefited
228 from the thin shell of HMIPs. Whatever HMIPs or HNIPs, they showed the lowest binding capacity to Sudan II,
229 the possible reason was the poor structural planarity of Sudan II hindered its adsorption.

230 (Fig. 4)

231 3.5 Analysis of chilli powder samples

232 A SPE-HPLC method was developed to determine Sudan I in chilli powder samples, which could attain
233 favorable limits of detection (LOD) of 4.0 $\mu\text{g kg}^{-1}$ based on the signals as 3-fold the baseline noise under the
234 optimal conditions (shown in experimental). Chilli powder samples spiked with different amount of Sudan I at 0, 4,
235 10 and 100 $\mu\text{g kg}^{-1}$ were determined and the results were shown in Table 4. A blank experiment was done with the
236 same procedures to evaluate the template leakage. As seen, the template of Sudan I had been removed completely.
237 Sudan I was found in the real chilli powder samples to be 7.0 $\mu\text{g kg}^{-1}$. For the spiked chilli powder samples
238 recoveries ranged from 95-108% were obtained with high precision (RSD<5%). The typical Chromatograms (Fig.
239 S4, ESI[†]) were shown for standard solution of Sudan I (a), a real chilli sample after the treatment of HMIPs (b)
240 and without the treatment of HMIPs for the same sample (c).

241 (Table 4)

242 (Fig. S4)

243 3.6 Regeneration studies of HMIPs.

244 The regeneration of HMIPs was considered to have a great cost benefit on extending their applications. A
245 HMIPs-SPE cartridge was repeated for usage to investigate the reuse capacity. After each use, the cartridge was
246 washed by methanol-acetic acid solution 90:10 (v/v) and methanol. Six cycles were performed and no less
247 recovery was found. The HMIPs were taken out for SEM images and the images before and after usage were
248 compared (Fig. S5, ESI[†]). It could be seen that after six cycles, the imprinting shell was still stable without broken.

249 (Fig. S5)

250 4. Conclusion

251 A novel strategy was successfully developed to prepare HMIPs, in which introduced both soft PS core and hard
252 SiO₂ inner shell with the help of sulfonation of PS, which ensured to obtain the solid and thinner MIPs shell.
253 Thinner MIPs shell provided fast mass transfer rate and the residual SiO₂ offered the support for increasing the
254 rigidness of MIPs. The HMIPs could be used repeatedly as SPE sorbent at least 6 times without decreasing the
255 adsorption capacity and being broken. It was expected to be used to enrich Sudan I from the complex samples.

256 Acknowledgements

257 The authors thank the fund supporting of the National Natural Science Foundation of China (No. 21375052) and
258 Gansu Province Science and technology support program (1204FKCA127) and Major Project (1102FKDA011)
259 and the Main Nature Science Foundation of Gansu Province in China (No.3ZS041-A25-009).

260 Notes and references

261 ^aState Key Laboratory of Applied Organic Chemistry, Lanzhou University, Lanzhou 730000, P. R. China

262 ^bTesting Demonstration Center for Food quality & safety of the Ministry of Industry & Information, Lanzhou 730000, P. R. China

263 *Corresponding author: Jiang He, Tel.: +86 (931) 891 2591, Fax: +86 (931) 891 2582, E-mail: hejiang@lzu.edu.cn

264 [†] Electronic Supplementary Information (ESI) available: The structures of Sudan dyes; Characterization and performance
265 evaluation results of HMIPs.

266 1 G. Wulff, A. Sarhan, *Angew. Chem., Int. Ed.*, 1972, 11, 341.

267 2 Y.K. Lu, X.P. Yan, *Anal. Chem.*, 2004, 76, 453.

- 1
2
3 268 3 G.Z. Fang, J. Tan, X.P. Yan, *Anal. Chem.*, 2005, 77, 1734.
4 269 4 D.M. Han, G.Z. Fang, X.P. Yan, *J. Chromatogr. A*, 2005, 1100, 131.
5 270 5 H.F. Wang, Y.Z. Zhu, X.P. Yan, R.Y. Gao, J.Y. Zheng, *Adv. Mater.*, 2006, 18, 3266.
6 271 6 P. Manesiotis, S. Kashani, P. McLoughlin, *Anal. Methods*, 2013, 5, 3122.
7 272 7 E. Piletska, D. Cowieson, C. Legge, A. Guereiro, K. Karim, S. Piletsky, *Anal. Methods*, 2013, 5, 6954.
8 273 8 S. F. Xu, J. H. Li and L. X. Chen, *J. Mater. Chem.*, 2011, 21, 4346.
9 274 9 L.X. Chen, S.F. Xua, J.H. Li, *Chem. Soc. Rev.*, 2011, 40, 2922.
10 275 10 Y. Tominaga, T. Kubo, K. Yasuda, K. Kato, K. Hosoya, *Micropor. Mesopor. Mat.*, 2012, 156, 161.
11 276 11 D. Gao, Z. P. Zhang, M. H. Wu, C. G. Xie, G. J. Guan, and D. P. Wang, *J. Am. Chem. Soc.*, 2007, 129, 7859.
12 277 12 Z. Zhang, S.F. Xu, J.H. Li, H. Xiong, H.L. Peng, L.X. Chen, *J. Agric. Food Chem.*, 2012, 60, 180.
13 278 13 S.F. Xu, L.X. Chen, J.H. Li, W. Qin, J.P. Ma, *J. Mater. Chem.*, 2011, 21, 12047.
14 279 14 G.J. Guan, Z.P. Zhang, Z.Y. Wang, B.H. Liu, D.M. Gao, C.G. Xie, *Adv. Mater.*, 2007, 19, 2370
15 280 15 X.B. Zhang, J. Li, B. You, G.P. Yong, H.W. Tong and S.M. Liu, *RSC Adv.*, 2012, 2, 9778.
16 281 16 J. Li, X.B. Zhang, Y.X. Liu, H.W. Tong, Y.P. Xu, S.M. Liu, *Talanta*, 2013, 117, 281.
17 282 17 W.Z. Xu, W. Zhou, P.P. Xu, J.M. Pan, X.Y. Wu, Y.S. Yan, *Chem. Eng. J.*, 2011, 172, 191.
18 283 18 W.M. Yang, L.K. Liu, W. Zhou, W.Z. Xu, Z.P. Zhou, W.H. Huang, *Appl. Surf. Sci.*, 2012, 258, 6583.
19 284 19 Y.C. Fan, M.L. Chen, S.T. Chao, F. El-Sepai, K.X. Wang, Y. Zhu, M.L. Ye, *Anal. Chim. Acta.*, 2009, 650, 65.
20 285 20 X.F. Gao, H.Y. Liu, Z.H. Song, X.L. He, F.X. Dong, *Spectroscopy*, 2007, 21, 135.
21 286 21 E. Ertaş, H. Özer, C. Alasalvar, *Food Chem.*, 2007, 105, 756.
22 287 22 W.C. Shan, J.Z. Xi, J. Sun, Y.J. Zhang, J.P. Wang, *Food Control*, 2012, 27, 146.
23 288 23 C. Yu, Q. Liu, L. Lan, B. Hu, *J. Chromatogr. A*, 2008, 1188, 124
24 289 24 L.M. He, Y.J. Su, B.H. Fang, X.G. Shen, Z.L. Zeng, Y.H. Liu, *Anal. Chim. Acta.*, 2007 594 139.
25 290 25 P. Qi, T. Zeng, Z.J. Wen, X. Liang, X.W. Zhang, *Food Chem.*, 2011, 15, 1462.
26 291 26 Y.T. Zhang, Z.J. Zhang, Y.H. Sun, *J. Chromatogr. A*, 2006, 1129, 34.
27 292 27 C.V.D. Anibal, M. Odena, I. Ruisánchez, M.P. Callao, *Talanta*, 2009, 79, 887.
28 293 28 X.G. Hu, Q.L. Cai, Y.N. Fan, T.T. Ye, Y.J. Cao, C.J. Guo, *J. Chromatogr. A*, 2012, 1219, 39.
29 294 29 S. Wang, Z.X. Xu, G.Z. Fang, Z.J. Duan, *J. Agric. Food Chem.*, 2007, 55, 3869.
30 295 30 H.Y. Yan, H. Wang, J.D. Qiao, G.L. Yang, *J. Chromatogr. A*, 2011, 1218, 2182.
31 296 31 F. Puoci, C. Garreffa, F. Iemma, R. Muzzalupo, U.G. Spizzirri, N. Picci, *Food Chem.* 2005, 93 349.
32 297 32 H.Y. Yan, J.D. Qiao, H. Wang, G.L. Yang, K.H. Row, *Analyst*, 2011, 136, 2692.
33 298 33 C.D. Zhao, T. Zhao, X.Y. Liu, H.X. Zhang, *J. Chromatogr. A*, 2010, 1217, 6995.
34 299 34 X.M. Feng, C.J. Mao, G. Yang, W.H. Hou, J.J. Zhu, *Langmuir*, 2006, 22, 4384.
35 300 35 J. Tan, M. Li, R. Li, Z.T. Jiang, *Anal. Methods*, 2013, 5, 1245.
36 301 36 S. Yang, Y.Z. Wang, M.L. Xu, M.Z. He, M. Zhang, D. Ran, X.P. Jia, *Anal. Methods*, 2013, 5, 5471.
37 302 37 H. Sertchook, D. Avnir, *Chem. Mater.*, 2013, 15, 1690.
38 303 38 K.G. Neoh, M.Y. Pun, E.T. Kang, K.L. Tan, *Synthetic Met.*, 1995, 73, 209.
39 304 39 H. Zeng, Y.Z. Wang, C. Nie, J.H. Kong, X.J. Liu, *Analyst*, 2012, 137, 2503.
40 305 40 J.M. Pan, H. Hang, X.H. Dai, J.D. Dai, P.W. Huo, Y.S. Yan, *J. Mater. Chem.*, 2012, 22, 17167.
41 306 41 X.T. Shen, T.C. Zhou, L. Ye, *Chem. Commun.*, 2012, 48, 8198.
42 307

308 Figure captions

309 Scheme 1. Schematic illustration of the preparation process of HMIPs.

310 Fig. 1. TEM images (A-C) and SEM images (a-c) of PS/SiO₂, MHSiO₂, and HMIPs.

311 Fig. 2. Adsorption isotherm of HMIPs and HNIPs for Sudan I in ACN. Experimental conditions: v=2.0 mL; mass
312 of polymers, 20 mg; adsorption time, 24 h.

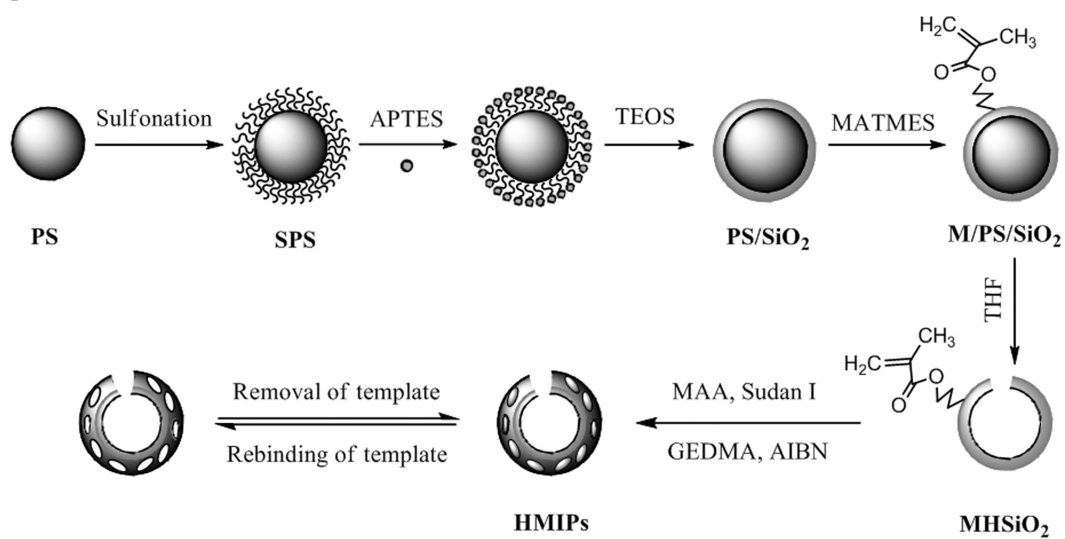
313 Fig. 3. Kinetic uptake of Sudan I onto the HMIPs and HNIPs. Experimental conditions: v=20 mL; mass of
314 polymers, 200 mg.

315 Fig. 4. Uptake of different Sudan dyes at the same initial concentration of 0.40 μmol mL⁻¹. Experimental
316 conditions: solvent, ACN; v=2 mL; mass of polymers, 20 mg; adsorption time, 1 h; structure references, Sudan
317 I-IV.

318
319
320
321
322
323
324
325
326

327

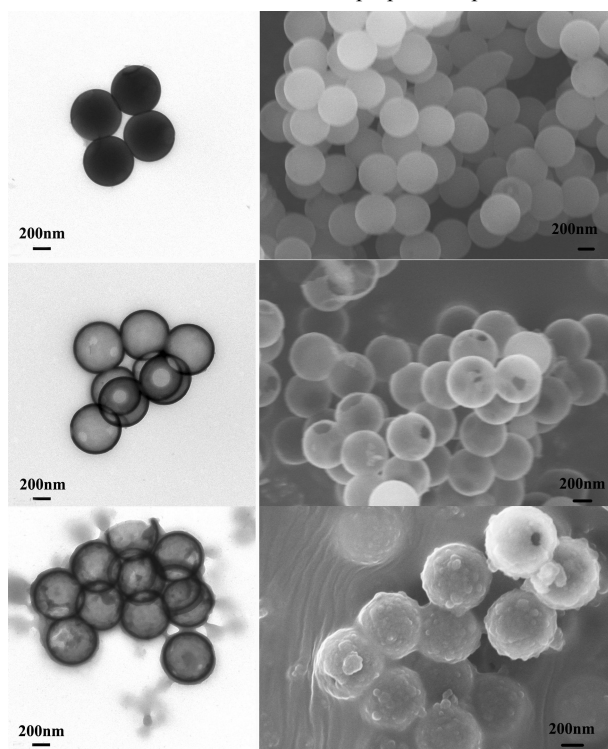
328 Captions



329

330

Scheme 1. Schematic illustration of the preparation process of HMIPs.



331

332

Fig. 1. TEM images (A-C) and SEM images (a-c) of PS/SiO₂, MHSiO₂, and HMIPs.

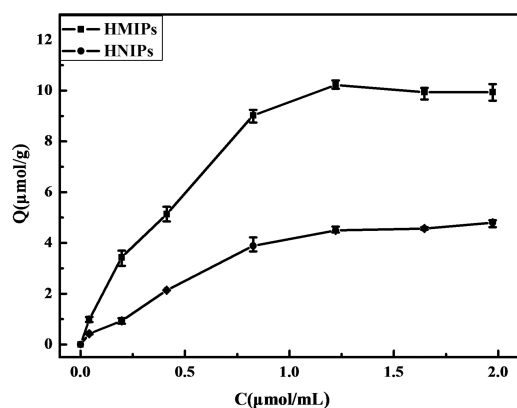


Fig. 2. Adsorption isotherm of HMIPs and HNIPs for Sudan I in ACN. Experimental conditions: $v=2.0$ mL; mass of polymers, 20 mg; adsorption time, 24 h.

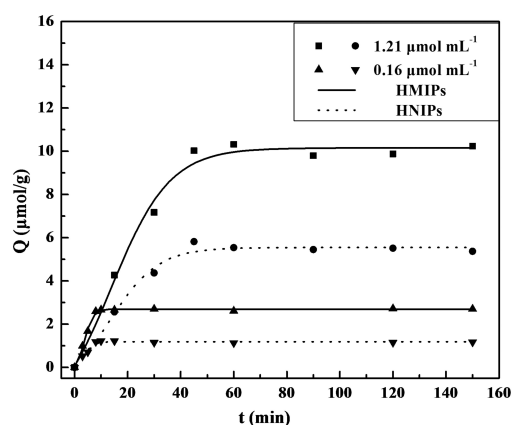


Fig. 3. Kinetic uptake of Sudan I onto the HMIPs and HNIPs. Experimental conditions: $v=20$ mL; mass of polymers, 200 mg.

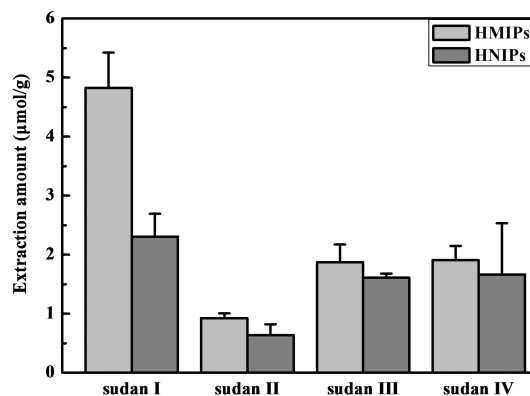


Fig. 4. Uptake of different Sudan dyes at the same initial concentration of $0.40 \mu\text{mol mL}^{-1}$. Experimental

342 conditions: solvent, ACN; $v=2$ mL; mass of polymers, 20 mg; adsorption time, 1 h; structure references, Sudan
343 I-IV.

344
345
346 Table 1. Comparison of the adsorption capacities of materials synthesized in different solvents
347

Solvent	^a 0.80 $\mu\text{mol mL}^{-1}$			^a 1.20 $\mu\text{mol mL}^{-1}$			^a 1.60 $\mu\text{mol mL}^{-1}$		
	Q_{HMIPs}	Q_{HNIPs}	α	Q_{HMIPs}	Q_{HNIPs}	α	Q_{HMIPs}	Q_{HNIPs}	α
Toluene	9.03	3.88	2.33	10.22	4.49	2.27	9.94	4.57	2.18
Chloroform	5.71	4.68	1.22	7.41	4.66	1.59	7.13	4.37	1.63

348 Q : $\mu\text{mol g}^{-1}$, $\alpha=Q_{\text{HMIPs}}/Q_{\text{HNIPs}}$. Amount of materials:20 mg; solvent: 2mL of ACN; adsorption time: 60 min; room
349 temperature. ^ainitial concentration of Sudan I.

350
351
352
353 Table 2. Isotherm model constants for HMIPs and HNIPs
354

Materials	Langmuir			Freundlich		
	R^2	Q_{max}	K_L	R^2	K_F	n
HMIPs	0.990	12.5	2.58	0.996	10.4	1.51
HNIPs	0.989	6.94	1.19	0.987	4.05	1.39

355
356
357
358
359 Table 3. Comparison of morphological stability and mass transfer of HMIPs with reported
360

Template molecule	Sacrificed core	Shell thickness (nm)	Morphological stability	^a adsorption capacity ($\mu\text{mol nm}^{-1}$)	mass transfer		Ref.
					Concentration of template ($\mu\text{mol mL}^{-1}$)	equilibration times (min)	
Sudan I	PS	500	Stable	0.014	0.16	40	12
Atrazine	PS	500	Stable	0.022	0.19	60	13
bisphenol A	SiO_2	80	crush	5.6	0.5	50	16
dibenzothiophene	TiO_2	/	crush	-	2.7	240	17
Dibenzothiophene	K_2TiO_4	/	crush	-	0.54	60	18
Sudan I	PS	50	Stable	0.25	0.5	25	this
					0.16	10	work

361 ^a adsorption capacity: adsorption amount on 1 nm of HMIP thickness.
362
363
364
365

1
2
3
4
5
6
7
8
9
10
11
12
13
14
15
16
17
18
19
20
21
22
23
24
25
26
27
28
29
30
31
32
33
34
35
36
37
38
39
40
41
42
43
44
45
46
47
48
49
50
51
52
53
54
55
56
57
58
59
60366
367

Table 4. Recoveries of Sudan I in chilli powder samples (n=3).

Chilli powder (g)	Sudan I added ($\mu\text{g kg}^{-1}$)	Found ($\mu\text{g kg}^{-1}$)	Recoveries (%)	RSD (%)
0	-	Not found	-	-
2	0	7.0	-	5.8
2	4	11.3	107.5	3.0
2	10	16.9	99.0	1.8
2	100	102.9	95.9	1.1

368